MPI-PTh/96-73
IFT-96/17
hep-ph/9608416

arXiv:hep-ph/9608416v1 22 Aug 1996

Unravelling the $WW\gamma$ and WWZ Vertices at the Linear Collider: $\bar{\nu}\nu\gamma$ and $\bar{\nu}\nu\bar{q}q$ final states

Debajyoti Choudhury*

Max–Planck–Institut für Physik, Werner–Heisenberg–Institut, Föhringer Ring 6, 80805 München, Germany.

and

Jan Kalinowski† ‡

Institute of Theoretical Physics, Warsaw University, Hoża 69, 00-681 Warsaw, Poland.

ABSTRACT

We perform a detailed analysis of the processes $e^+e^- \to \bar{\nu}\nu\gamma$ and $\bar{\nu}\nu\bar{q}q$ at future linear e^+e^- colliders and assess their sensitivity to anomalous gauge boson couplings. We consider center of mass energies $\sqrt{s} = 350$, 500 and 800 GeV. We demonstrate that significant improvements can be obtained if the phase space information for the cross sections is used maximally. At 800 GeV the parameters $\Delta\kappa_\gamma$ and λ_γ can be constrained, at 95% CL, to about 0.02 and 0.01, while the parameters $\Delta\kappa_Z$, λ_Z and Δg_1^Z can be probed down to about 0.009, 0.002 and 0.004 respectively. The precision of these measurements is likely to be limited by statistical errors at anticipated luminosities at these energies.

*debchou@mppmu.mpg.de
†kalino@fuw.edu.pl
‡Supported in part by the Polish Committee for Scientific Research.

1 Introduction

Although the LEP and SLC measurements are often claimed to have vindicated the Standard Model (SM) at better than 1% level [1], in reality, this success has been limited to an accurate determination of the fermion-vector boson couplings. The nature of the vector boson self couplings, as yet, is only poorly measured. Thus, inspite of our prejudice for the 'gauge dogma', we are still far from establishing the W and the Z to be gauge bosons. On the other hand, even if we are to believe in the SM, we are led to another question. Is there a "great desert" beyond, or does new physics soon overwhelm the SM? Can (all) the particles associated with the new physics be discovered directly ? If not, can the existence of new thresholds cause significant departures in the vector boson self couplings? This seems quite likely in the light of the remarkable agreement between the direct measurement of the top quark mass and the indications from the precision measurements at LEP. A precise measurement of these vertices is thus of paramount importance.

Departures from the gauge theory prediction are, perhaps, best constrained from a consideration of the virtual effects that these engender in various low energy observables like the anomalous magnetic moment of the muon [2], rare meson decays [3] and the precision electroweak data [4]. However, such bounds suffer from the fact that they necessitate either an assumption of lack of any *cancellation* between various corrections, or a complete specification of the new physics scenario.

It is thus more attractive to measure such effects directly and, indeed, much effort has been directed towards this goal, both in the context of the forthcoming LEP2 operation [5], or the proposed Linear Colliders (LC) [6]. The W pair-production process has been studied in great detail as a probe for gauge boson self-couplings. In this article we argue that an additional set of measurements, at no extra cost, can and *should* be made at the LC in our quest of unravelling this sector of the SM. One of these ($e^+e^- \to \bar{\nu}\nu\gamma$) is sensitive solely to the $W^+W^-\gamma$ vertex while the other ($e^+e^- \to \bar{\nu}\nu\bar{q}q$) is sensitive primarily to the W^+W^-Z coupling. With the aditional knowledge that these measurements will provide, a *model independent* evaluation would be much easier to achieve.

In the next section, we review the generic triple vector boson vertex (TGV) and summarize current experimental limits and improvements that can be achieved at LEP2 and Tevatron. In Sec. 3 we argue for the case of $\bar{\nu}\nu\gamma$ and $\bar{\nu}\nu Z$ final states. They are then discussed in detail and expected experimental bounds are derived in the following two sections. Finally we summarize our conclusions in Sec. 6.

2 The Anomalous Couplings

New physics can, and, in general, will manifest itself in corrections to both the triple and the quartic vector boson vertex. We concentrate here, however, only on the former set. While quartic couplings can be investigated at the LC [6, 7], the expected bounds tend to be weaker. Furthermore, in an effective Lagrangian language, any operator that would

cause a modification in the quartic vertex without causing a corresponding one in the TGV, would be suppressed by higher powers of momentum.

Expressed in purely phenomenological terms, the effective Lagrangian for the $WW\gamma$ and the WWZ vertex can be expressed in terms of seven parameters each [8]. Of these seven, three violate CP while a fourth one violates C and P but conserves CP. As, pending large cancellations, data on the neutron electric dipole moment constrain these very severely [9], we shall not discuss them any further[4]. The effective Lagrangian, thus restricted, can be expressed as (with $V \equiv \gamma$ or Z)

$$\begin{aligned}\mathcal{L}_{\mathit{eff}}^{WWV} = \; & -ig_V\Big[\,(1+\Delta g_1^V)\left(W^\dagger_{\alpha\beta}W^\alpha - W^{\dagger\alpha}W_{\alpha\beta}\right)V^\beta + (1+\Delta\kappa_V)W^\dagger_\alpha W_\beta V^{\alpha\beta} \\ & + \frac{\lambda_V}{M_W^2}W^\dagger_{\alpha\beta}W^\beta{}_\sigma V^{\sigma\alpha}\Big]\end{aligned} \tag{1}$$

where $V_{\alpha\beta} = \partial_\alpha V_\beta - \partial_\beta V_\alpha$ and $W_{\alpha\beta} = \partial_\alpha W_\beta - \partial_\beta W_\alpha$. In eq. (1), g_V is the overall WWV coupling in the SM, *viz.*,

$$g_\gamma = e, \qquad g_Z = e\cot\theta_W \ , \tag{2}$$

where θ_W is the weak mixing angle. Electromagnetic gauge invariance requires that $\Delta g_1^\gamma(q^2=0) = 0$, though it can assume other values for off-shell photons, a fact often missed in the literature. Within the SM, we have, at the tree level,

$$\Delta g_1^\gamma = \Delta g_1^Z = \Delta\kappa_\gamma = \Delta\kappa_Z = \lambda_\gamma = \lambda_Z = 0 \ . \tag{3}$$

It is easy to see that eq.(1) is the most general expression consistent with Lorentz, C and P invariance. All higher derivative terms can be reabsorbed into the couplings above provided they are treated as form-factors and not constants. It is thus important to bear in mind the fact that the strength of the various terms in the vertex would vary (in general, independently) with the momentum scale of the process being considered.

To date, the only direct constraints are those obtained for κ_γ and λ_γ from an analysis of the $W\gamma$ events at the Tevatron [11]. The 95% C.L. bounds are

$$-1.6 < \Delta\kappa_\gamma < 1.8 \qquad \text{and} \qquad -0.6 < \lambda_\gamma < 0.6 \ . \tag{4}$$

It is also estimated that an analysis of the WW and WZ events in the Run 1b data will lead to bounds like $-0.65 < \Delta\kappa_\gamma < 0.75$ and $-0.4 < \lambda_{\gamma,Z} < 0.4$. Further improvements (approximately by a factor of 2) are expected if the main injector becomes operative [12].

In the context of the oncoming runs at LEP2, considerable efforts [5] have been made to determine the sensitivity of W^+W^- pair production (rate as well as phase space distribution) on the anomalous couplings with the conclusion: the individual bounds would be quite similar to those obtainable at the Tevatron, though the parameter space contours would be different. While LEP2 *might* do marginally better for $\Delta\kappa_{\gamma,Z}$, Tevatron is better poised[5] for constraining $\lambda_{\gamma,Z}$. At the LC however, the same process would lead to more than an order of magnitude improvement in the bounds [6]. Only then would we begin to probe the radiative corrections to these couplings expected within the SM [13] or the minimal supersymmetric standard model (MSSM) [14].

[4] In a collider, these operators are best isolated by looking at final state asymmetries [10].

[5] Since these represent higher dimensional operators, their contribution to the cross section increases with the center of mass energy, unless the couplings themselves decrease with the momentum transfer.

3 The Case for $\bar{\nu}\nu\gamma$ and $\bar{\nu}\nu Z$ Final States

It is quite obvious that compared to W-pair production, the processes being proposed here are suppressed by higher powers of g_V. Thus the cross sections are, naively, expected to be smaller. Furthermore, the invisibility of the neutrinos lead to considerable loss of information. This, then, points to a reduced sensitivity. Why therefore consider such final states at all? To appreciate this, one needs to recount that a process like $f\bar{f} \to W^+W^-$ receives contribution from both the γ– and the Z–mediated s-channel process. Thus, all of the six[6] $WW\gamma/Z$ couplings are inexorably intertwined. This leads to two possible difficulties. For one, it is quite conceivable that the new physics corrections to the couplings are such that their contributions to the W pair production cancel to a significant degree, thus reducing sensitivity. On the other hand, even if a deviation in the cross section is seen, this would not point us to a unique theory. These are critical issues as a measurement of the TGV at the LC could be a critical tool in examining radiative corrections within the SM or the MSSM.

There are two solution to the imbroglio. One is to consider experiments in different collider modes and combine the results obtained therein. For example, the cross sections for both $W\nu$ production in an $e\gamma$ collider [15] and W-pair production in $\gamma\gamma$ colliders [15] are independent of the WWZ vertex (as well as the form factor nature of g_1^γ). On the other hand, all the couplings do contribute to $We\nu$ production at an e^-e^- collider. However, the interplay being different, this mode can provide significant new information [16]. If one were not willing to consider another machine, the alternative would be to look for processes with different dependence on the anomalous couplings. Hadronic colliders have an advantage in that they permit many more potentially interesting modes. We already have mentioned three in the context of the Tevatron. Unfortunately, the sensitivity tends to be lower for the noncanonical final states.

At the canonical LC, inspite of the lower sensitivity expected, it is thus interesting to consider final states other than W^+W^-. The two simplest examples of this are provided by $\bar{\nu}\nu\gamma$ (sensitive only to $\Delta\kappa_\gamma$ and λ_γ, g_1^γ being unity as the photon is on-shell) and $\bar{\nu}\nu Z$ (sensitive to $\Delta\kappa_Z$, λ_Z and Δg_1^Z). Although both these processes have already been considered in the literature [17, 18, 19, 5], we bring into the analysis a greater degree of sophistication and demonstrate that such an experiment is actually much more sensitive than what was previously thought.

4 $e^+e^- \to \bar{\nu}\nu\gamma$

The signal here would be a single energetic photon accompanied by missing momentum (equal and opposite to that of the photon). While a significant fraction of such events would arise from $Z\gamma$ production, their importance can be reduced by appropriate kinematical cuts, as we shall demonstrate below. The relevant Feynman diagrams are shown in Fig. 1. Diagrams (1 & 2) form a gauge-invariant subset by themselves, and also lead

[6]Since the photon is off-shell, g_1^γ is no longer constrained to be unity.

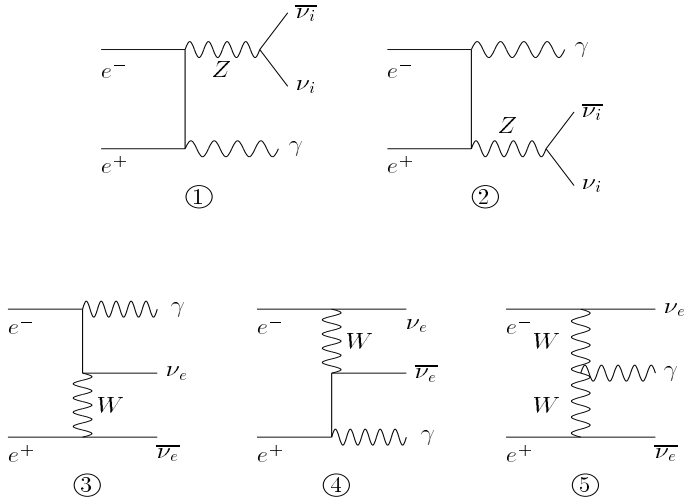


Figure 1: *The Feynman diagrams responsible for* $e^+e^- \to \bar{\nu}\nu\gamma$.

to $\bar{\nu}_\mu\nu_\mu\gamma$ and $\bar{\nu}_\tau\nu_\tau\gamma$ final states. The helicity amplitudes can be found in ref. [18]. Before examining the cross-sections, let us delineate first the kinematical cuts that we will employ. It is clear that bremsstrahlung-type diagrams lead, preferentially, to photons close to the beam axis. To enhance the importance of the TGV, it is thus necessary to impose an angular cut on the photon. We find

$$25^\circ < \theta_\gamma < 155^\circ \tag{5}$$

to be a suitable choice. Further, the photon must have sufficient energy to be detectable. We thus require

$$E_\gamma > 25\,\text{GeV}\ . \tag{6}$$

The above combination also implies that the events must have a missing transverse momentum $\not{p}_T > 10.6\,\text{GeV}$. This then takes care of the process $e^+e^- \to \gamma\gamma$ with one photon disappearing into the beam pipe. The SM production cross section with these cuts is presented in Fig. 2*a*. The increase in the rates with $\sqrt{s}$ is symptomatic of the diagram with the TGV[7]. Also shown in the figure is the cross-section for $\bar{\nu}_\mu\nu_\mu\gamma$ production. At a first glance, it might seem that the latter is an unimportant background. However, keeping in mind that these diagrams are operative for all three neutrino flavours, it is worthwhile to suppress this contribution, especially for lower energies. This is best done by realizing that diagrams 1 & 2 of Fig. 1 tend to populate phase space volume corresponding to a (nearly) real Z production and, hence, can be effectively eliminated by demanding that

$$\left| E_\gamma - \frac{s - m_Z^2}{2\sqrt{s}} \right| > 5\Gamma_Z\ , \tag{7}$$

where $\sqrt{s}$ is the centre of mass energy. This obviously means that the missing mass ($\not{m}$) is away from m_Z by more than $5\Gamma_Z$. With this additional cut, the total cross section

[7] Of course, gauge invariance does ensure partial wave unitarity, as can be explicitly checked.

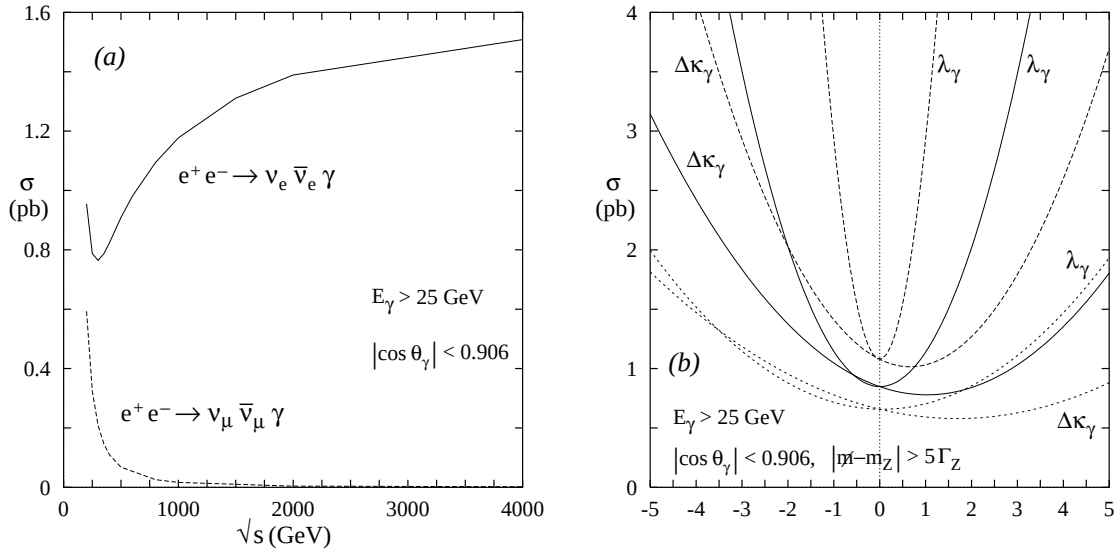


Figure 2: (a) *The variation of the SM cross sections with the center of mass energy; and* (b) *The total single photon cross section as a function of the individual anomalous couplings for a fixed center of mass energy (dotted : 350 GeV, solid : 500 GeV, dashed : 800 GeV). The other coupling is held to be vanishing.*

(summed over neutrino flavours) is

$$\sigma_{\rm SM}(\bar{\nu}\nu\gamma) = \begin{cases} 0.658\,{\rm pb} & \sqrt{s} = 350\,{\rm GeV} \\ 0.848\,{\rm pb} & \sqrt{s} = 500\,{\rm GeV} \\ 1.079\,{\rm pb} & \sqrt{s} = 800\,{\rm GeV}\ . \end{cases} \tag{8}$$

Switching on the anomalous couplings, we see immediately that the cross sections are rather sensitive to these. In Fig. 2*b* we show the cross section as a function of one anomalous coupling with the other equal to zero. The sensitivity increases with the center of mass energy (the effect, expectedly, being more pronounced for λ_γ) since deviations from the gauge theory prediction leads to a 'bad' high energy behaviour.

It is instructive to compare the figures in eq.(8) with those for $\sigma_{\rm SM}(W^+W^-)$, which decreases strongly with $\sqrt{s}$. In fact, the two are quite comparable for $\sqrt{s} \sim 800$ GeV. Consequently, the reduction in sensitivity on account of differences in cross section, becomes less and less severe as the center of mass energy increases. There is yet another feature that one should keep in mind. Unlike in W^+W^- production, the existence of an anomalous coupling affects primarily the high-energy end of the photon-spectrum. This very concentration allows one to tune the selection criteria and thereby maximize the sensitivity. This feature will also hold for $\bar{\nu}\nu Z$ case (Sec.5).

4.1 Deriving the constraints

The significant dependence of the total cross section (see Fig. 2*b*) on the TGV would tempt one to derive bounds from this alone, and this was the approach taken in refs.[17, 18].

However, using just the total cross section is tantamount to discarding a considerable amount of crucial information, as is illustrated dramatically in ref.[5]. Significant improvements can be expected if the phase space information can be used maximally. While many sophisticated algorithms like the maximum likelihood method or use of the optimal variables exist, we desist from using these. Rather, we choose a simple χ^2 test. Dividing the phase space into an adequate number of bins, we define

$$\chi^2 = \sum_{i=1}^{\text{bins}} \left| \frac{N_{SM}(i) - N_{anom}(i)}{\Delta N_{SM}(i)} \right|^2 \ , \tag{9}$$

where N_{SM} and N_{anom} are, respectively, the number of events predicted within the SM and a theory with an anomalous TGV. To calculate the number of events, we choose, for the integrated luminosity, two typical design values for each choice of center of mass energy

$$\mathcal{L} = \begin{cases} 10,\ 25 & \text{fb}^{-1} & \sqrt{s} = 350\ \text{GeV} \\ 20,\ 50 & \text{fb}^{-1} & \sqrt{s} = 500\ \text{GeV} \\ 50,\ 120 & \text{fb}^{-1} & \sqrt{s} = 800\ \text{GeV} \ . \end{cases} \tag{10}$$

The error in eq. (9) is a combination of statistical and systematic errors

$$\Delta N = \sqrt{(\sqrt{N})^2 + (\delta_{syst} N)^2} \ . \tag{11}$$

Since the neutrinos are invisible, the only phase space information available is the energy and emergence angle of the photon : $(E_\gamma, \cos\theta_\gamma)$. Working with this set, we divide the phase space consistent with the cuts of eqs.(5–7) into 40×40 equal sized bins. It might be argued that we have resorted to an extremely fine binning, especially since cross sections are not very large. However, the bins are not populated evenly. A large fraction of the events are concentrated in relatively few bins, leaving the other almost empty. To prevent spurious contributions from the latter, we discount any bin with less than one event. We have also checked that the results do not have a very strong dependence on bin cardinality.

Since both the emergence angle and the energy of the photon should be measurable to a very great accuracy (particularly within the restricted phase space that we consider), the main systematic errors originate from the luminosity measurement and from detector efficiencies. Since these should not exceed 1%, we conservatively assume an overall systematic uncertainty of 2%, *i.e.* $\delta_{syst} = 0.02$ in eq.(11). The error, for the most part, is thus dominated by the statistical fluctuations. In Fig. 3, we present the $\chi^2 = 6$ contours in the $\Delta\kappa_\gamma$–λ_γ plane for the configurations of eq.(10). The interpretation of the figure is simple. The areas of the parameter space lying outside each contour can be ruled out with 95% confidence respectively. If only one of the parameters is of interest, irrespective of the values taken by the other, the half-planes beyond the edges of the contours can be ruled out at 98.6% C.L. If one of the parameters is known to take its SM value, the latter confidence levels are valid for the half-lines bounded by the intersections of the contours with the axis. Several comments are in order:

- Assuming the other coupling to be identically zero, the prospective 95% C.L. bounds

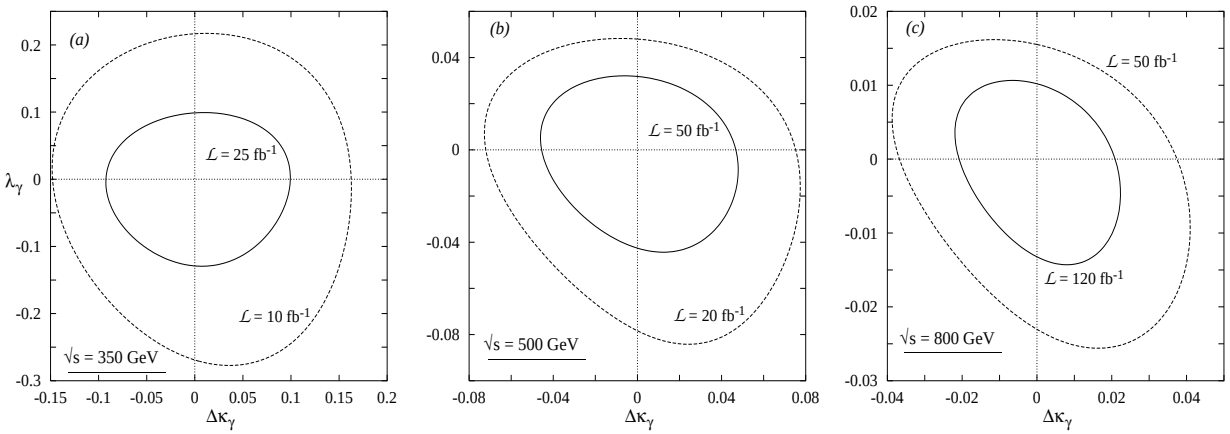


Figure 3: $\chi^2 = 6$ *contours in the* $\Delta\kappa_\gamma$–λ_γ *plane for various collider configurations. The cuts of (5–7) have been imposed and* 40×40 *bins in* $(\cos\theta_\gamma, E_\gamma)$ *used.*

are

$$\begin{aligned} -0.074 < \Delta\kappa_\gamma < 0.079, \quad -0.100 < \lambda_\gamma < 0.091, \qquad & \text{for } (350\,\text{GeV}, 20\,\text{fb}^{-1}) \\ -0.036 < \Delta\kappa_\gamma < 0.037, \quad -0.033 < \lambda_\gamma < 0.026, \qquad & \text{for } (500\,\text{GeV}, 50\,\text{fb}^{-1}) \\ -0.017 < \Delta\kappa_\gamma < 0.017, \quad -0.010 < \lambda_\gamma < 0.0083, \qquad & \text{for } (800\,\text{GeV}, 120\,\text{fb}^{-1}) \end{aligned} \tag{12}$$

These bounds are one order of magnitude better than those obtained in ref. [18] from a consideration of total cross section alone.

- The bounds on λ_γ improve much faster with the available center of mass energy than those on $\Delta\kappa_\gamma$.

- Although not as strong as the bounds expected from W^+W^- production, the present ones compare well. In fact, those obtainable at the larger $\sqrt{s}$ would probe radiative corrections within the MSSM [14].

- The contours tilt only slightly with respect to the axes, showing that there is very little correlation between the two parameters $\Delta\kappa_\gamma$ and λ_γ.

- Harnessing possible beam polarization is an intriguing thought. Two things need to be remembered though. Since the kinematical cuts have already eliminated most of the contribution from the Z–mediated diagrams (including the interference terms), beam polarization affects all relevant diagrams equally. Thus only a quantitative change in the contours can be expected. This is in marked contrast to the case in the e^-e^- case [16], where experiments with different beam polarization settings complement each other. Secondly, only left handed polarization would be useful[8]. Explicit computation with a 90% left polarized beam and the same luminosity shows about 15% improvement in the bounds.

- We have not incorporated initial state radiation effects, which may affect performance somewhat.

[8]Thus, if the machine runs only part of the time with a left-polarized beam, the bounds will suffer.

5 $e^+e^- \to \bar{\nu}\nu Z$

At the first sight, this is very similar to the case considered in the previous section, but for the fact that one needs to consider additional diagrams with the Z radiated from a neutrino. A similar decomposition to gauge invariant subsets may be done. Although the expressions for the helicity amplitudes are a little more complicated owing to the considerable mass of the Z, these exist in the literature [19]. Apparently, all that remains to be done is to convolute the said expressions with the corresponding decay ($Z \to f\bar{f}$) matrix amplitudes so as to obtain the relevant final states. However, such an approximation is valid only in the limit of exact mass reconstruction. Since this is unlikely to be as accurate at the LC as at LEP1, one needs to consider non-resonant production as well. This leads us, inexorably, to the full $e^+e^- \to \nu\bar{\nu}f\bar{f}$ matrix elements for various choices of f.

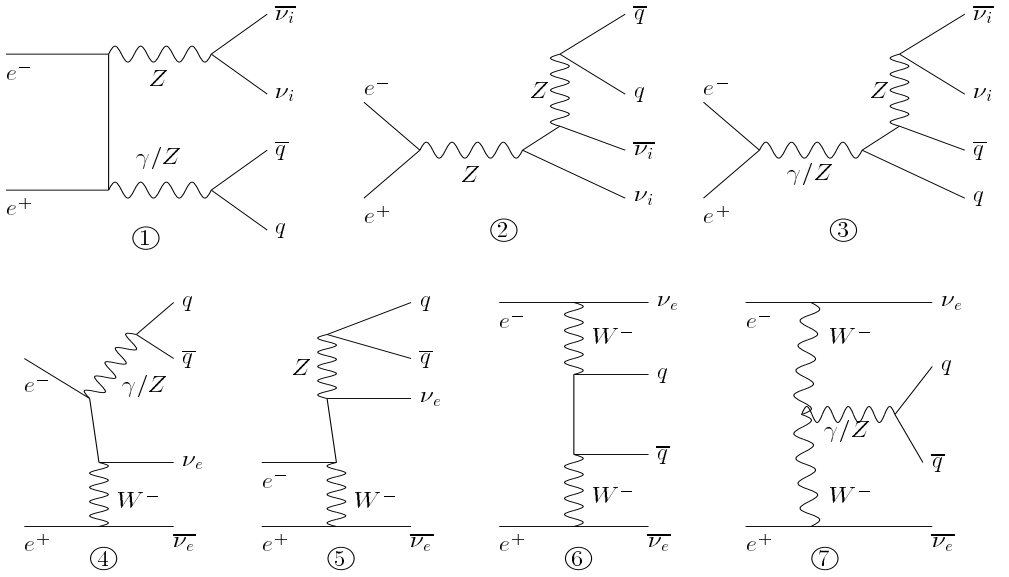


Figure 4: *The different topology classes for Feynman diagrams responsible for* $e^+e^- \to \bar{\nu}\nu\bar{q}q$.

The Feynman diagrams can be divided into different topology classes and in Fig. 4, we exhibit the seven classes for $f = q$. Of the 19 diagrams, four each are of types 1,3 & 4, two each of types 2,5 & 7 and finally one of type 6. The diagrams of type 3 and type 6 would be missed if one had calculated only $e^+e^- \to \bar{\nu}\nu Z$. Again, types 1–3 constitute a gauge-invariant subset and contribute to all three neutrino flavours, while types 4–7 are operative for the electron neutrino only. The diagram of interest is then of type 7. Note that all six (including g_1^γ) of the couplings in eq.(1) can contribute. Does this, then, give a lie to our claims of the separability of $WW\gamma$ and WWZ couplings? We shall show below that this is not the case. Indeed, the kinematical cuts that we will adopt will render the cross section to be very insensitive to the $WW\gamma$ vertex. Consequently, any appreciable deviation from that source could only occur for very large values of $\Delta\kappa_\gamma$ (or λ_γ) and thus can be ruled out by the experiment described in the previous section. This of course does not hold for Δg_γ^1. However, with the aforementioned cuts, the experiment is sensitive only to $\Delta g_\gamma^1 \sim \mathcal{O}(10)$, and thus this particular form factor can safely be assumed to be

vanishing in the course of our analysis.

To calculate the diagrams we use an appropriately modified form of the helicity amplitude package MadGraph [20]. Extensive counterchecks were performed both through explicit calculations as well as with CompHEP [21].

5.1 The signal and the kinematical cuts

We choose, in this analysis, to restrict ourselves to $f = q$. Apart from the fact that the associated cross section is much larger than that for $f = e, \mu, \tau$, this has other advantages too. Each of the last three final states also receive contribution from additional Feynman diagrams, the most important being W pair-production. As the latter involves both the $WW\gamma$ and the WWZ vertex (and that too for a different q^2 value), it defeats the avowed objective of our analysis[9].

The signal is thus 2 jets accompanied by large missing momentum. For the jets to be detectable, we require that they have sufficient energy and be sufficiently away from the beam pipe, *viz.*,

$$E_j > 20\,\mathrm{GeV}, \quad 20^\circ < \theta_j < 160^\circ \ . \tag{13}$$

Further, to ensure that the event selection criteria do not merge the two jets into a single jet, we demand that the jet-jet angular separation be large enough [23] :

$$\theta_{jj} > 20^\circ \ . \tag{14}$$

To enrich the the $\bar{\nu}\nu Z$ component of the event sample, we require that the jet-jet invariant mass be sufficiently close to m_Z :

$$|m_{jj} - m_Z| < 3\Gamma_Z \ . \tag{15}$$

This removes, to a very large extent, the contribution from diagram (6), and from those of diagrams (1,2,4,7) where the exchanged boson is the photon. We need to ensure that the missing momentum arises on account of a $\bar{\nu}\nu$ pair. Therefore, we demand that the missing momentum ($\not{p}$) have a large enough transverse component and that its rapidity be small enough :

$$\not{p}_T > 40\,\mathrm{GeV}, \qquad \eta(\not{p}) < 1 \ . \tag{16}$$

This, for example, eliminates processes such as $e^+e^- \to \bar{q}q\gamma$ with the photon vanishing into the beam pipe. Finally, to eliminate the contributions from diagrams of the types (1–3), we require that the missing mass ($\not{m} \equiv \sqrt{\not{p}^{\,2}}$) be sufficiently away from m_Z :

$$|\not{m} - m_Z| > 5\Gamma_Z \ . \tag{17}$$

In Fig.5, we display the variation of SM cross section for the $\bar{\nu}_e\nu_e\bar{q}q$ process with the center of mass energy after the cuts (13–17) have been imposed. As in the case of $\bar{\nu}_e\nu_e\gamma$ cross section, it shows a slow increase with $\sqrt{s}$, a characteristic of the t-channel diagram

[9] The $\mu^+\mu^-\nu\bar{\nu}$ final state has, however, been analysed in ref.[22].

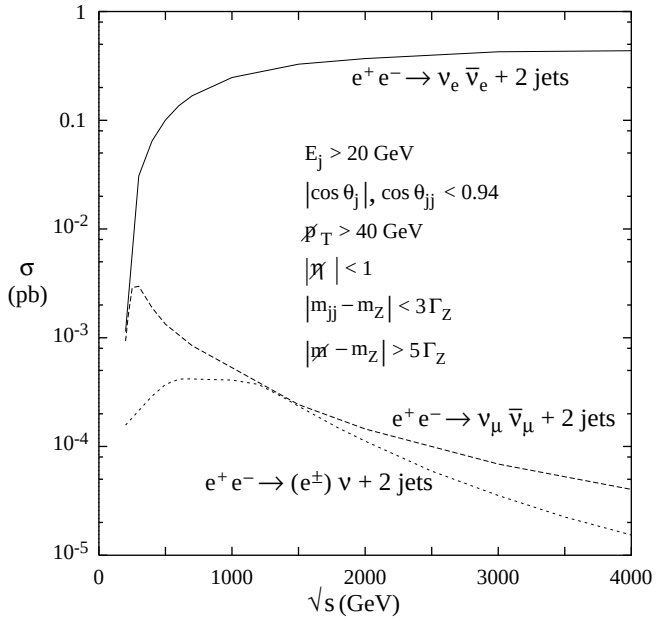


Figure 5: *The variation of the SM cross section with the center of mass energy.*

with the TGV. While our cross sections are understandably different from those of ref.[19], we have checked that we reproduce their result in the proper limit. Also shown in the Fig.5 is the $\bar{\nu}_\mu \nu_\mu \bar{q} q$ cross section. As expected, this is much smaller (the cut eq.(17) plays a crucial role) and decreases with the center of mass energy. The total SM cross-section for the $\bar{\nu}\nu\bar{q}q$ (*i.e.*, summed over neutrino and quark flavours) is thus

$$\sigma_{\rm SM}(\bar{\nu}_i \nu_i \bar{q} q) = \begin{cases} 51.88\,\text{fb} & \sqrt{s} = 350\,\text{GeV} \\ 103.6\,\text{fb} & \sqrt{s} = 500\,\text{GeV} \\ 198.4\,\text{fb} & \sqrt{s} = 800\,\text{GeV}\ . \end{cases} \tag{18}$$

We have, until now, not considered other (potentially irreducible) SM backgrounds to our signal. The most important of these is the process

$$e^+e^- \to l^\mp \overset{(-)}{\nu_l}\, \bar{q} q' \tag{19}$$

with the charged lepton moving down the beam pipe. Understandably, $l = e$ is the main culprit. We determine the corresponding cross section within the equivalent photon approximation (with any $e^\mp$ within an angle of 10° of the beam considered to be invisible). The cuts in eqs.(15 & 16) play an important role in reducing this cross section, and were partially designed keeping this in mind. The resultant cross section is displayed in Fig.5 and is seen to be quite innoccuos.

As soon as the anomalous couplings are switched on, the cross sections change appreciably (see Fig.6). As expected, the deviation is larger for higher center of mass energies, with the steepest change occurring for λ_Z. While Ambrosanio & Mele (ref.[19]) derived their bounds essentially from plots corresponding to those in Fig.6, we shall attempt to

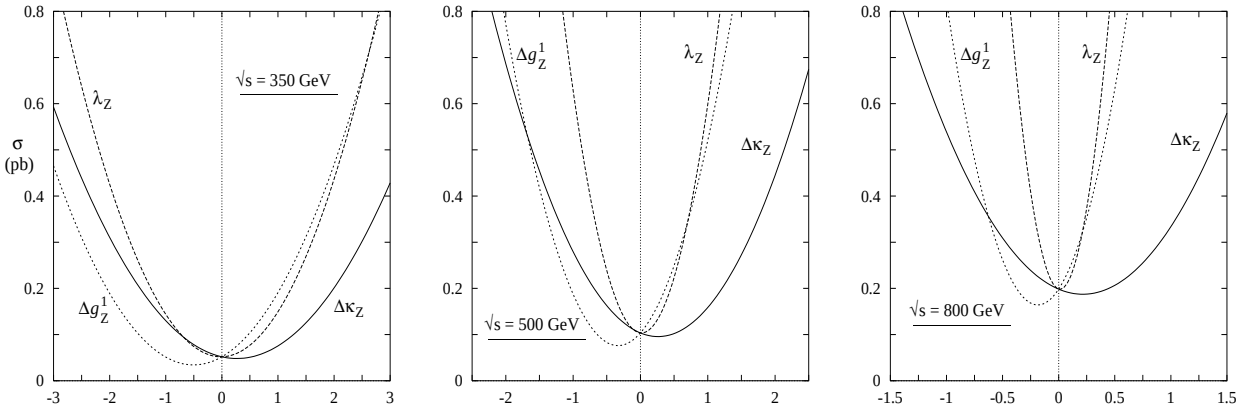


Figure 6: *The variation of the total cross section with individual anomalous couplings (the others being zero). The cuts (13–17) have been imposed.*

extract more information from the phase space distribution of the events. To this end, we can follow the procedure of section 4.1. The situation here is more complicated though. For one, we have three anomalous couplings instead of two and the constant χ^2 surfaces are thus two-dimensional. Secondly, unlike the case in the previos section, we now have quite a few independent phase space variables. Consequently, we could, in principle, attempt a more detailed fitting.

We shall, nonetheless, set ourselves a much simpler goal. Instead of attempting a multivariable fit (which would take us close to the maximum likelihood method), we shall restrict ourselves to simpler 2-dimensional distributions (*i.e.*, distributions in two independent kinematical variables), with an effort to identify best such pair for each detector configuration. We again use eqs.(9 & 11) to calculate the χ^2. Furthermore, rather than presenting the constant–χ^2 ellipsoids, we shall only present their projections on each co-ordinate plane. The interpretation is then akin to that of section 4.1 with the constraint that the third coupling is identically vanishing.

5.2 The constraints

As the cross sections are significantly smaller than those in section 4, we adopt coarser binnings, especially for the lower energy options. While distributions in different kinematical variables are sensitive to the three couplings to different extent, we have restricted ourselves to one particular pairing for each $\sqrt{s}$, our choice being

$$\begin{aligned}
\sqrt{s} = 350\,\mathrm{GeV} \;&:\; (min(|\cos\theta_1|, |\cos\theta_2|), E_1 + E_2) && 20 \times 20 \text{ bins}\,, \\
\sqrt{s} = 500\,\mathrm{GeV} \;&:\; (min(|\cos\theta_1|, |\cos\theta_2|), \text{corresponding } E_i) && 30 \times 30 \text{ bins}\,, \\
\sqrt{s} = 800\,\mathrm{GeV} \;&:\; (max(|\cos\theta_1|, |\cos\theta_2|), \text{corresponding } E_i) && 40 \times 40 \text{ bins}\,,
\end{aligned} \tag{20}$$

where the subscripts refer to the jets. In Figs.7(a–i) we display the 95% C.L. exclusion contours for the three different pairings of the anomalous couplings. The interpretation is the same as in section 4.1.

The main conclusions can be summarised as follows :

- Assuming the other two couplings to be identically zero, the 95% C.L. bounds, for typical $(\sqrt{s}/\mathrm{GeV}, \mathcal{L}/\mathrm{fb}^{-1})$ combinations, would be

$$\begin{aligned}
(350, 25): &\quad -75 < \overline{\Delta\kappa_Z} < 90, \quad -104 < \overline{\lambda_Z} < 79, \quad -40 < \overline{\Delta g_1^Z} < 37, \\
(500, 50): &\quad -35 < \overline{\Delta\kappa_Z} < 38, \quad -5.6 < \overline{\lambda_Z} < 5.5, \quad -15 < \overline{\Delta g_1^Z} < 14, \qquad (21) \\
(800, 120): &\quad -10 < \overline{\Delta\kappa_Z} < 9.9, \quad -2.1 < \overline{\lambda_Z} < 2.1, \quad -4.3 < \overline{\Delta g_1^Z} < 4.2,
\end{aligned}$$

where $\overline{\Delta\kappa_Z} \equiv \Delta\kappa_Z/1000$ etc.

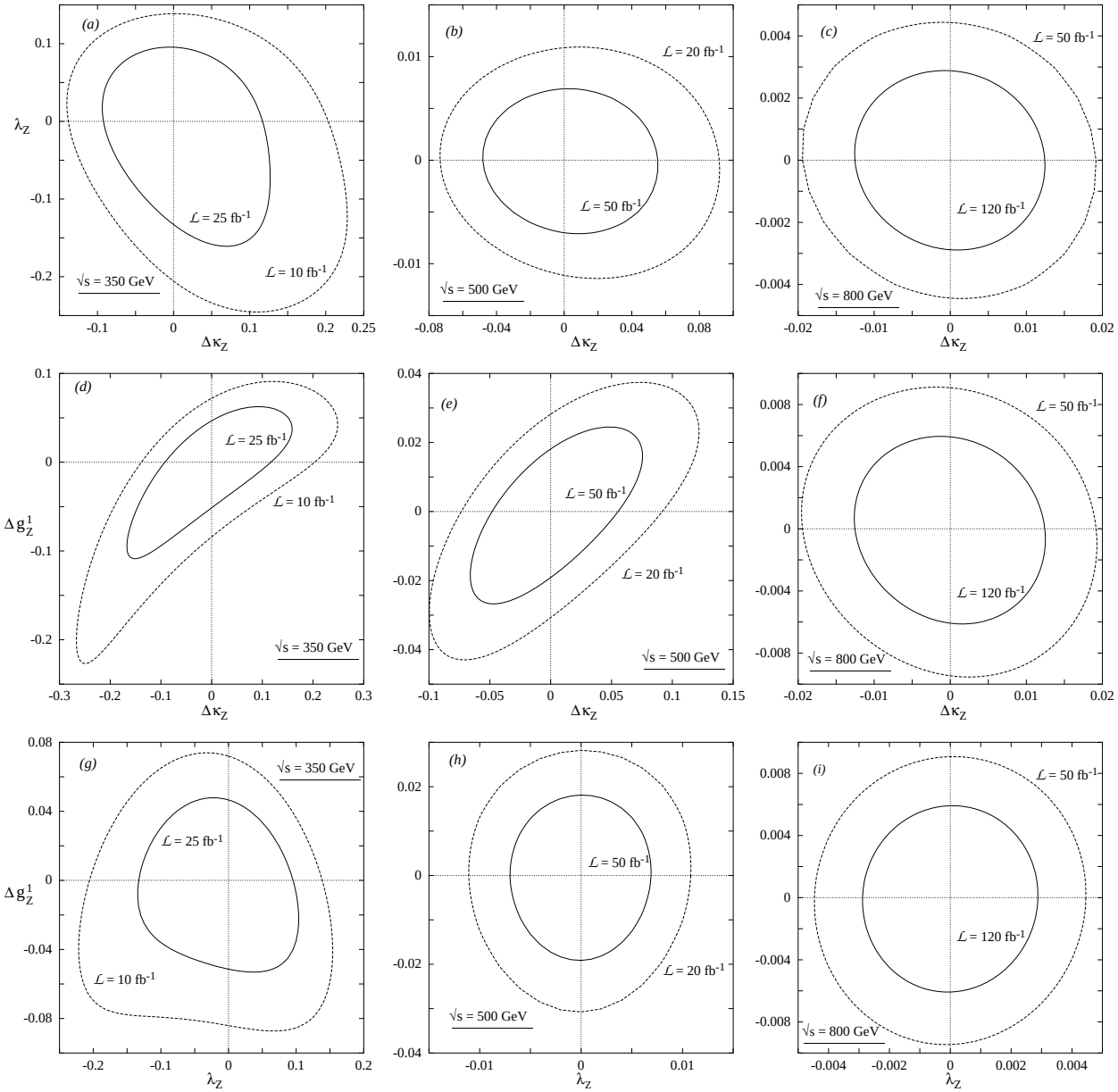


Figure 7: *Projections of the $\chi^2 = 6$ contours on the three coordinate planes for various collider configurations. The cuts (13–17) have been imposed and the binnings of eq.(20) adopted.* (a–c) *on $\Delta\kappa_Z$–λ_Z plane;* (d–f) *on $\Delta\kappa_Z$–Δg_1^Z plane;* (g–i) *on λ_Z–Δg_1^Z plane.*

- The bounds are thus quite comparable to those expected from W pair production at the same machine. Exploration of radiative contributions to this vertex thus becomes possible.
  The second generation machines (higher center of mass energy and luminosity) will lead to a significant improvement in the constraints, with the largest improvement occuring for the λ_Z.

- The most discernible correlations are for the $(\Delta\kappa_Z, \Delta g_1^Z)$ pair. This is to be expected as $\Delta g_1^Z = \Delta\kappa_Z$ implies that only the overall WWZ coupling has been changed.
  This correlation disappears for higher $\sqrt{s}$ as the non-gauge nature of the theory becomes more apparent.

- Inclusion of the initial state radiation effects (neglected in this analysis) is expected to degrade the results somewhat. On the other hand, the use of the full phase space information (whether maximum likelihood or optimal variables) can be expected to improve the bounds.

- As in section 4.1, beam polarization is not a priority.

6 Summary

We have shown that the processes $e^+e^- \to \bar{\nu}\nu\gamma$ and $\bar{\nu}\nu Z(\to \bar{q}q)$ can be very useful in disentangling the anomalous $WW\gamma$ and WWZ couplings. We have included all tree level processes that lead to these final states. The signal to background ratio is improved by imposing a set of kinematical cuts. Contrary to naive expectations, the relevant cross sections are not severely suppressed in comparison with those for W-pair-production. In addition, the effect of possible anomalous couplings is concentrated largely in the high-energy end of the γ ($\bar{q}q$) spectrum thus allowing for a more efficient extraction of information.

Exploiting the full phase space knowledge of the cross sections, one can derive bounds that are comparable to those expected from W^+W^- production. Apart from disentangling the $WW\gamma$ and the WWZ couplings, this measurement has the added advantage of being performed at a different momentum transfer. Coupled with the W^+W^- measurements, these then offer the possibility of studying the form-factor nature of these couplings.

Acknowledgements : We would like to thank R. Settles, G. Wilson and P.M. Zerwas for many discussions and continous encouragement. JK thanks M. Krawczyk for useful discussion and help.

References

[1] ALEPH, DELPHI, L3 and OPAL collaborations, CERN-PPE-94-187, Nov 1994;
The LEP Electroweak Working Group, CERN preprint LEPEWWG/96-28 (1996).

[2] S.J. Brodsky and J.D. Sullivan, *Phys. Rev.* **156** (1967) 1644;
F. Herzog, *Phys. Lett.* **B148** (1984) 355, (E) *Phys. Lett.* **B155** (1985) 468;
A. Grau and J.A. Grifols, *Phys. Lett.* **B154** (1985) 283;
J.C. Wallet, *Phys. Rev.* **D32** (1985) 813;
P. Méry, S.E. Moubarik, M. Perrottet, and F.M. Renard, *Zeit. für Physik* **C46** (1990) 229;
F. Boudjema, K. Hagiwara, C. Hamzaoui, and K. Numata, *Phys. Rev.* **D43** (1991) 2223.

[3] S.P. Chia, *Phys. Lett.* **B240** (1990) 465;
K. Numata, *Zeit. für Physik* **C52** (1991) 691;
K.A. Peterson, *Phys. Lett.* **B282** (1992) 207;
T.G. Rizzo, *Phys. Lett.* **B315** (1993) 471;
U. Baur, Proc. *"Workshop on B Physics at Hadron Accelerators"*, Snowmass, Colorado, June 1993, p. 455;
X. He and B. McKellar, *Phys. Lett.* **B320** (1994) 165;
R. Martinez, M.A. Pérez, and J.J. Toscano, *Phys. Lett.* **B340** (1994) 91;
M.S. Alam *et al.*, (CLEO Collaboration), *Phys. Rev. Lett.* **74** (1995) 2885;
G. Baillie, *Zeit. für Physik* **C61** (1994) 667.

[4] A. de Rujula, M.B. Gavela, P. Hernandez and E. Masso, *Nucl. Phys.* **B384** (1992) 3;
K. Hagiwara, S. Ishihara, R. Szalapski and D. Zeppenfeld, *Phys. Lett.* **B283** (1992) 353; *Phys. Rev.* **D48** (1993) 2182;
J.J. van der Bij, *Phys. Lett.* **B296** (1992) 239.

[5] G. Gounaris *et al.*, (hep-ph/9601233), in *Report of the Workshop on Physics at LEP2*; CERN Yellow Report 96-01, eds. G. Altarelli, T. Sjostrand and F. Zwirner.

[6] G. Bélanger and F. Boudjema, *Proc. Munich, Annecy, Hamburg Workshop, e^+e^- Collisions at 500 GeV* (1991) ed. P.M. Zerwas;
J. Kalinowski, same proc; *Acta Phys. Polon.* **B23** (1992) 1237.

[7] F. Cuypers, *Phys. Lett.* **B344** (1995) 369.

[8] J.F. Gaemers and G.J. Gounaris, *Zeit. für Physik* **C1** (1979) 259;
K. Hagiwara, R.D. Peccei and D. Zeppenfeld, *Nucl. Phys.* **B282** (1987) 253.

[9] W. J. Marciano and A. Queijeiro, *Phys. Rev.* **D33** (1986) 3449.

[10] H.S. Mani, B. Mukhopadhyaya and S. Raychaudhuri, M.R.I, Allahabad preprint MRI-PHY/9/93 (1993);
D. Chang, W.-Y. Keung and I. Phillips, *Phys. Rev.* **D48** (1993) 4045.

[11] F. Abe *et al.*(CDF Collaboration), *Phys. Rev. Lett.* **74** (1995) 1936; *Phys. Rev. Lett.* **75** (1995) 1017;
S. Abachi *et al.*(D0 Collaboration), *Phys. Rev. Lett.* **75** (1995) 1023; *Phys. Rev. Lett.* **75** (1995) 1034.

[12] H. Aihara *et al.*, Summary of the *Working Subgroup on Anomalous Gauge Boson Interactions* of the DPF Long Range Planning Study, report FERMILAB-Pub-95/031 (1995).

[13] G. Couture *et al.*, *Phys. Rev.* **D36** (1987) 859;
J. Papavassiliou and K. Philippides, *Phys. Rev.* **D48** (1993) 4255;
E.N. Argyres *et al.*, *Nucl. Phys.* **B391** (1993) 23;
see also the references cited in [14].

[14] A.B. Lahanas and V.C. Spanos, *Phys. Lett.* **B334** (1994) 378; hep-ph/9504340;
E.N. Argyres, A.B. Lahanas, C.G. Papadopoulos and V.C. Spanos, hep-ph/9603362;
A. Arhrib, J.-L. Kneur and G. Moultaka, *Phys. Lett.* **B376** (1996) 127; hep-ph/9603268.

[15] S.Y. Choi and F. Schrempp, *Phys. Lett.* **B272** (1991) 149;
E. Yehudai, *Phys. Rev.* **D44** (1991) 3434.

[16] D. Choudhury and F. Cuypers, *Phys. Lett.* **B325** (1994) 50; *Nucl. Phys.* **B429** (1994) 33.

[17] G. Couture and S. Godfrey, *Phys. Rev.* **D50** (1994) 5607.

[18] K.J. Abraham, J. Kalinowski and P. Sciepko, *Phys. Lett.* **B339** (1994) 136.

[19] S. Ambrosanio and B. Mele, *Nucl. Phys.* **B374** (1992) 3.

[20] T. Stelzer and F. Long, *Comput. Phys. Commun.* **81** (1994) 357.

[21] E. Boos *et al.*, in: *New Computing Techniques in Physics Research*, eds. D. Perret-Gallix and W. Wojcik, Paris, 1990, p. 573.

[22] G. Couture and S. Godfrey, *Phys. Rev.* **D49** (1994) 5709.

[23] R. Settles, private communication.